



**HAL**  
open science

## Combining F-18-DOPA PET and MRI with perfusion-weighted imaging improves delineation of high-grade subregions in enhancing and non-enhancing gliomas prior treatment: a biopsy-controlled study

Antoine Girard, Pierre-Jean Le Reste, Alice Metais, Beatrice Carsin Nicol, Dan Cristian Chiforeanu, Elise Bannier, Boris Campillo-Gimenez, Anne Devillers, Xavier Palard-Novello, Florence Le Jeune

### ► To cite this version:

Antoine Girard, Pierre-Jean Le Reste, Alice Metais, Beatrice Carsin Nicol, Dan Cristian Chiforeanu, et al.. Combining F-18-DOPA PET and MRI with perfusion-weighted imaging improves delineation of high-grade subregions in enhancing and non-enhancing gliomas prior treatment: a biopsy-controlled study. *Journal of Neuro-Oncology*, 2021, 155 (3), pp.287-295. 10.1007/s11060-021-03873-w . hal-03412994

**HAL Id: hal-03412994**

**<https://hal.science/hal-03412994>**

Submitted on 22 Nov 2021

**HAL** is a multi-disciplinary open access archive for the deposit and dissemination of scientific research documents, whether they are published or not. The documents may come from teaching and research institutions in France or abroad, or from public or private research centers.

L'archive ouverte pluridisciplinaire **HAL**, est destinée au dépôt et à la diffusion de documents scientifiques de niveau recherche, publiés ou non, émanant des établissements d'enseignement et de recherche français ou étrangers, des laboratoires publics ou privés.



Distributed under a Creative Commons Attribution - NonCommercial 4.0 International License

[Click here to view linked References](#)

## Clinical Study

### Title

Combining  $^{18}\text{F}$ -DOPA PET and MRI with perfusion-weighted imaging improves delineation of high-grade subregions in enhancing and non-enhancing gliomas prior treatment: a biopsy-controlled study

### Authors

Antoine GIRARD, MD; Pierre-Jean LE RESTE, MD; Alice METAIS, MD; Beatrice CARSIN NICOL, MD; Dan Cristian CHIFOREANU, MD; Elise BANNIER, PhD; Boris CAMPILLO-GIMENEZ, MD; Anne DEVILLERS, MD; Xavier PALARD-NOVELLO, MD, PhD; Florence LE JEUNE, MD, PhD

### Affiliations

Department of Nuclear Medicine, Eugène Marquis Center, Rennes, France (A.G., A.D., X.PN., F.LJ.)

Department of Neurosurgery, Rennes University Hospital, Rennes, France (P.J.LR.)

Department of Pathology, Rennes University Hospital, Rennes, France (A.M., DC.C.)

Department of Radiology, Rennes University Hospital, Rennes, France (B.CN., E.B)

Empenn IRISA research team, Rennes University-CNRS-INRIA-INSERM, Rennes, France (E.B.)

Department of Medical Oncology, Eugène Marquis Center, Rennes, France (B.CG.)

Signal and Image Processing Laboratory (LTSI), INSERM-University of Rennes 1, Rennes, France (A.G., X.PN, F.LJ., B.CG.)

### Corresponding Author

Dr Antoine GIRARD

ORCID: 0000-0002-9472-9980

Nuclear Medicine Department, Centre Eugène Marquis, Avenue de la Bataille Flandres-Dunkerque, 35000 Rennes, France

Phone: +33 2 99 25 30 00 Fax: +33 2 99 25 31 55

Email: [a.girard@rennes.unicancer.fr](mailto:a.girard@rennes.unicancer.fr)

**Author's contribution:**

Conceptualization: Antoine GIRARD, Pierre-Jean LE RESTE, PALARD-NOVELLO, Florence LE JEUNE

Methodology: Antoine GIRARD, Boris CAMPILLO-GIMENEZ, Elise BANNIER, Florence LE JEUNE

Formal analysis and investigation: Antoine GIRARD, Pierre-Jean LE RESTE, Alice METAIS, Beatrice

CARSIN NICOL, Dan Cristian CHIFOREANU,

Writing - original draft preparation: Antoine GIRARD, Pierre-Jean LE RESTE, Xavier PALARD-NOVELLO

Writing - review and editing: Anne DEVILLERS, Florence LE JEUNE

Funding acquisition: Xavier PALARD-NOVELLO, Florence LE JEUNE

Resources: Dan Cristian CHIFOREANU, Elise BANNIER, Anne DEVILLERS, Xavier PALARD-NOVELLO

Supervision: Florence LE JEUNE

**Acknowledgments**

MRI data acquisition was performed at the Neurinfo MRI research facility (Rennes I University-Rennes

University Hospital-INRIA-CNRS-Rennes Cancer Center). Neurinfo is also supported by Brittany Regional

Council, Rennes Metropole, and GIS IBISA.

## Abstract

**Purpose:** We aimed to compare spatial extent of high-grade subregions detected with combined [<sup>18</sup>F]-dihydroxyphenylalanine (<sup>18</sup>F-DOPA) PET and MRI to the one provided by advanced multimodal MRI alone including contrast-enhanced (CE) and perfusion weighted imaging (PWI). Then, we compared the accuracy between imaging modalities, in a per biopsy analysis.

**Methods:** Participants with suspected diffuse glioma were prospectively included between June 2018 and September 2019. Volumes of high-grade subregions were delineated respectively on <sup>18</sup>F-DOPA PET and MRI (CE and PWI). Up to three per-surgical neuronavigation-guided biopsies were performed per patient.

**Results:** Thirty-eight biopsy samples from sixteen participants were analyzed. Six participants (38%) had grade IV IDH wild-type glioblastoma, six (38%) had grade III IDH-mutated astrocytoma and four (24%) had grade II IDH-mutated gliomas. Three patients had intratumoral heterogeneity with coexisting high- and low-grade tumor subregions. High-grade volumes determined with combined <sup>18</sup>F-DOPA PET/MRI (median of 1.7 [interquartile range (IQR) 0.0,19.1] mL) were larger than with multimodal MRI alone (median 1.3 [IQR 0.0,12.8] mL) with low overlap (median Dice's coefficient 0.24 [IQR 0.08,0.59]). Delineation volumes were substantially increased in five (31%) patients. In a per biopsy analysis, combined <sup>18</sup>F-DOPA PET/MRI detected high-grade subregions with an accuracy of 58% compared to 42% (p=0.03) with CE MRI alone and 50% (p=0.25) using multimodal MRI (CE+PWI).

**Conclusions:** The addition of <sup>18</sup>F-DOPA PET to multimodal MRI (CE and PWI) enlarged the delineation volumes and enhanced overall accuracy for detection of high-grade subregions. Thus, combining <sup>18</sup>F-DOPA with advanced MRI may improve treatment planning in newly diagnosed gliomas.

**Key Words:** Positron-Emission Tomography; Glioma; Magnetic Resonance Imaging; Perfusion Weighted Imaging

## Text

### Introduction

Gliomas are the most common primary malignant brain tumors in adults. Extent of tumor resection is one of the most important prognostic factors [1]. Beyond the purposes of histological diagnosis, surgical resection serves to remove as much of the tumor as is safely achievable, while preventing new permanent neurological deficits [2]. Nevertheless, in these highly heterogeneous tumors with possible coexistence of high- and low-grade subregions, neoplastic cells diffusely infiltrate the brain far beyond the tumor core, and gliomas cannot be cured surgically [1–4]. Presurgical identification of high-grade subregions extent is of major importance, as it may influence the risk-benefit assessment determining the extent of tumor resection and ensure accurate pathological diagnosis.

MRI with and without contrast agent injection is currently the imaging method of reference for revealing high-grade glioma (HGG) subregions [2]. However, approximately one third of nonenhancing gliomas are malignant [5], and one quarter of low-grade gliomas show contrast enhancement (CE) [6]. Furthermore, in these heterogeneous tumors, CE extent does not always reflect all the HGG extent. Several neuroimaging tools have been developed to detect nonenhancing HGG burden, such as perfusion-weighted imaging (PWI) and amino-acid PET [7, 8]. PWI is extensively used to characterize gliomas at diagnosis [9]. Based on dynamic susceptibility contrast imaging, regional cerebral blood volume (rCBV) maps are calculated, highlighting neoangiogenesis suggestive of HGG transformation [10]. Amino-acid PET, including [ $^{18}\text{F}$ ]-fluoro-ethyl-tyrosine ( $^{18}\text{F}$ -FET), [ $^{11}\text{C}$ ]-methionine and [ $^{18}\text{F}$ ]-dihydroxyphenylalanine ( $^{18}\text{F}$ -DOPA) PET, has been increasingly investigated in the past decade and is the subject of recent guidelines [8, 11, 12]. We hypothesized that  $^{18}\text{F}$ -DOPA PET and multimodal MRI (with CE and PWI) complement each other to detect and define spatial extend of HGG prior treatment, and that combined interpretation of multimodal MRI and  $^{18}\text{F}$ -DOPA PET improves accuracy for detection of brain areas with HGG infiltration.

In the present study, we aimed, in patients with newly suspected gliomas, to evaluate whether adding  $^{18}\text{F}$ -DOPA PET to multimodal MRI (with CE and PWI) substantially modified delineation volumes of high-grade subregions. Then, we compared accuracy between imaging modalities, in a per biopsy analysis.

### Materials and methods

## Study participants

Between June 2018 and September 2019, we prospectively included consecutive participants with newly suspected supratentorial diffuse glioma (World Health Organization (WHO) Grades II-IV) referred to our institution for surgical resection. Included participants had to be at least 18 years old and covered by national health insurance. Exclusion criteria were pregnancy, emergency situations, and carbidopa, catechol-O-methyl transferase inhibitor, haloperidol or reserpine medication, as well as the absence of biopsy or surgical resection. All participants provided their written informed consent. This study was validated by an institutional review board and registered as a clinical trial (NCT03525080). Data generated or analyzed during the study are available from the corresponding author by request.

## <sup>18</sup>F-DOPA PET/CT protocol

<sup>18</sup>F-DOPA was produced via nucleophilic route by Curium Pharma (France) with a mean specific activity of 500 GBq/μmol. After at least 4 hours' fasting, participants were slowly injected with 2MBq/kg of <sup>18</sup>F-DOPA intravenously, without carbidopa premedication. A 20-minute PET data acquisition session was conducted 10 minutes after injection with a Biograph mCT Flow (Siemens Healthineers, Erlangen, Germany) integrated PET/CT system, in accordance with current recommendations [11]. PET images were reconstructed with attenuation correction, without point-spread function correction, using a fully 3D ordered-subset expectation maximization algorithm (8 iterations and 21 subsets) with a 400 x 400, matrix, 1 x 1 x 2 mm<sup>3</sup> voxel size. A Gaussian 3D kernel of 3 mm full width at half maximum was applied.

## MRI protocol

Data acquisition was performed on a Magnetom Prisma 3T (Siemens Healthineers, Erlangen, Germany), and included 3D-T1 MPRAGE-weighted imaging before and 6.5 minutes after gadolinium-based contrast agent (gadoteric acid) injection (repetition time (TR) = 1900 ms; inversion time (TI) = 900 ms; echo time (TE) = 2.26 ms), and dynamic susceptibility contrast PWI (TR = 1250 ms; TE = 30 ms). Corrected rCBV images were calculated with the DSCoMAN plugin (Duke University) in ImageJ v.1.52a (NIH). CE images were obtained by registering and subtracting T1-weighted images without contrast from those obtained after contrast agent injection. Fluid attenuated inversion recovery (FLAIR) weighted images were also performed.

## Surgical resections and biopsies

1 Surgeries were performed under general anesthesia by a senior neurosurgeon (P.J.L.R.), with the aid of  
2 neuronavigation from StealthStation S7 (Medtronic, Dublin, Ireland) based on morphological MRI. Up to three  
3 per-surgical neuronavigation-guided biopsies were performed per participant, depending on the tumor size. To  
4 avoid multiple burr holes, biopsies were performed after craniotomy, but before durotomy, with Sedan needles,  
5 to limit brain-shift. Biopsy targets were previously selected according to a consensus agreement between the  
6 neurosurgeon and the nuclear medicine physician. All biopsies were located in areas of FLAIR hyperintensity.  
7  
8 With the aim to identify imaging characteristics to differentiate high-grade and low-grade subregions, biopsies  
9 sites were targeted both in areas with and without imaging characteristics of HGG ( $^{18}\text{F}$ -DOPA increased uptake,  
10 contrast enhancement and neoangiogenesis). Imaging characteristics of each biopsy site are detailed in  
11 Supplementary Material 1.  
12  
13  
14  
15  
16  
17  
18  
19  
20

## 21 Pathology

22  
23 Each resection specimen and biopsy sample was collected, prepared and analyzed blind to imaging by  
24 two certified pathologists (A.M. and DC.C.). Samples were prepared using standard histopathological techniques.  
25  
26 Diagnosis and grading were performed on formalin-fixed paraffin-embedded tissue sections stained by  
27 hematoxylin and eosin, using complementary techniques to detect isocitrate dehydrogenase (IDH) mutation and  
28 1p19q codeletion, in accordance with the WHO 2016 Classification of Tumors of the Central Nervous System  
29 [13]. Each resection specimen and biopsy sample was graded independently. If grades were heterogeneous  
30 between samples from the same tumor, the WHO tumor grade was based on the highest-grade component.  
31  
32  
33  
34  
35  
36  
37  
38

## 39 Image analysis

40  
41 Image processing and analysis were performed using MIPAV v7.4.0 (NIH) by a senior nuclear medicine  
42 physician (A.G.) and a senior radiologist (B.CN.). PET and MRI images were post hoc registered for each  
43 participant, and the perfect spatial correspondence was visually checked. A reference area was drawn on one  
44 slice including the whole normal contralateral hemisphere at the centrum semiovale level.  $^{18}\text{F}$ -DOPA PET images  
45 were normalized by the maximum standardized uptake value of the reference area. Based on these normalized  
46 uptake images,  $^{18}\text{F}$ -DOPA PET high-grade subregions volumes ( $^{18}\text{F}$ -DOPA<sub>VOI</sub>) were defined semi-automatically  
47 as including all voxels with a tumor-to-brain ratio (TBR) higher than 1.7, in accordance with previously published  
48 data [14]. For MRI, CE<sub>VOI</sub> included all the voxels with a signal higher than the mean signal of the reference area  
49 + two standard deviations, and rCBV<sub>VOI</sub> were defined with a threshold of 1.6 times the mean signal of the  
50 reference area [15]. For each defined volume, signals related to noise or normal structures were manually  
51  
52  
53  
54  
55  
56  
57  
58  
59  
60  
61  
62  
63  
64  
65

1 removed (e.g., striatum in  $^{18}\text{F}$ -DOPA PET, and blood vessels in CE and rCBV images). Two additional volumes  
2 were defined respectively as  $\text{MRI}_{\text{VOI}}$  the union of  $\text{CE}_{\text{VOI}}$  and  $\text{rCBV}_{\text{VOI}}$ , and  $^{18}\text{F}$ -DOPA/ $\text{MRI}_{\text{VOI}}$  the union of  $^{18}\text{F}$ -  
3  $\text{DOPA}_{\text{VOI}}$  and  $\text{MRI}_{\text{VOI}}$ . Biopsy sites were located on images based on neuronavigational data as 1mL cubic  
4 volumes. Defined tumor volumes of at least one voxel were required for tumors and/or biopsy sites to be  
5 considered positive (+) respectively for each image series.  
6  
7  
8  
9

## 10 **Statistical analysis**

11  
12  
13 Statistical analysis was performed with MedCalc® version 12.5.0.0 (Medcalc Software bvba, Ostend,  
14 Belgium). Volumes regarded as high-grade tumor infiltration were described as median and inter-quartile range  
15 (IQR). Tumor volumes were considered substantially different between imaging modalities if they varied of more  
16 than 2 mL, or switched from null to non-null. Volumes overlaps were described using the Dice similarity  
17 coefficient (DSC). Diagnostic performances are reported with their 95% confidence intervals (95% CI) and were  
18 compared pairwise with the McNemar t-test. Uptake ratios and pathological features were compared with the  
19 Mann-Whitney non-parametric test. An alpha risk of 0.05 was considered indicative of statistical significance.  
20  
21  
22  
23  
24  
25  
26  
27  
28  
29  
30

## 31 **Results**

### 32 **Participants and tumors**

33  
34  
35  
36  
37 Nineteen participants were prospectively included. Three were excluded because they didn't undergo  
38 both targeted biopsy and surgical resection. For two of these participants surgeries were performed in other  
39 hospitals, and for one participant biopsies alone were preferred to surgical resection. Sixteen participants and 38  
40 biopsy samples were therefore considered for the analysis (Fig. 1). Participants and tumors characteristics are  
41 presented in Table 1. Median age was 40 [IQR 27, 55] years, with an M/F sex ratio of 10/6 (63%). The median  
42 interval between PET and MRI was 3 [IQR 2, 7] days, and the median delay between PET and surgery was 15  
43 [IQR 14, 36] days.  
44  
45  
46  
47  
48  
49  
50

### 51 **Tumor imaging characteristics and volumes**

52  
53  
54 High-grade tumor volumes defined with each imaging modality are presented in Table 2. High-grade  
55 volumes determined with combined  $^{18}\text{F}$ -DOPA PET and multimodal (CE + PWI) MRI ( $^{18}\text{F}$ -DOPA/ $\text{MRI}_{\text{VOI}}$ ) were  
56 larger than with multimodal (CE + PWI) MRI ( $\text{MRI}_{\text{VOI}}$ ) alone, with medians of 1.7 [IQR 0.0, 19.1] mL and 1.3  
57  
58  
59  
60  
61  
62  
63  
64  
65

1 [IQR 0.0, 12.8] mL, respectively. When measurable (positive with both modalities involved), median overlap  
2 calculated with DSC was 0.24 [IQR 0.08, 0.59] between  $^{18}\text{F}$ -DOPA<sub>VOI</sub> and MRI<sub>VOI</sub>, 0.28 [IQR 0.17, 0.58]  
3 between  $^{18}\text{F}$ -DOPA<sub>VOI</sub> and CE<sub>VOI</sub>, 0.27 [IQR 0.03, 0.53] between  $^{18}\text{F}$ -DOPA<sub>VOI</sub> and rCBV<sub>VOI</sub>, and 0.24 [IQR  
4 0.00, 0.40] between CE<sub>VOI</sub> and rCBV<sub>VOI</sub>.  
5  
6

7  
8 Adding  $^{18}\text{F}$ -DOPA PET to multimodal MRI (with CE and PWI) substantially impacted delineation of  
9 high-grade tumor volumes in 5 out of 16 (31%) patients. It raised (> 2 mL) volumes in 3 out of 7 (43%)  
10 participants with enhancing glioma (participants 01, 08 and 10), and in 1 out of 9 (11%) with non-enhancing  
11 tumor (participant 19). Moreover,  $^{18}\text{F}$ -DOPA PET revealed HGG infiltration in 1 out of 7 (14%) non-enhancing  
12 HGG without neoangiogenesis on PWI (participant 05). There was neither MRI(+)/ $^{18}\text{F}$ -DOPA(-) HGG, nor  $^{18}\text{F}$ -  
13 DOPA(+) low-grade glioma. Main patterns of HGG with multimodal  $^{18}\text{F}$ -DOPA PET/MRI are shown in Fig. 2.  
14  
15  
16  
17  
18  
19  
20

### 21 **Multimodal imaging diagnostic performance, in a per biopsy analysis**

22  
23 All the 38 biopsy samples analyzed corresponded to cellular glioma tissue, 5 (13%) samples were WHO  
24 Grade IV glioma, 24 (63%) were Grade III, and 9 (24%) were Grade II. Five (31%) tumors were found with  
25 intratumoral heterogeneous grades with coexisting grades: II/III for two tumors, II/IV for one tumor, and III/IV  
26 for two tumors.  
27  
28  
29  
30  
31

32  
33 Diagnostic performance of each imaging modality is presented in Table 3. Adding  $^{18}\text{F}$ -DOPA PET to multimodal  
34 MRI (with CE and PWI) led to correctly identify three more HGG subregions from three different participants,  
35 providing an accuracy of 58% compared to 50% with multimodal MRI alone (p=0.25). Sensitivity was 52%  
36 versus 41% (p=0.25), respectively, and specificity of 78% for both (p=1.00).  $^{18}\text{F}$ -DOPA/MRI provided  
37 significantly higher accuracy than CE MRI alone that was 42% (p=0.03), which had a sensitivity of 28% (p=0.02)  
38 and a specificity of 89% (p=1.00).  
39  
40  
41  
42  
43  
44  
45  
46  
47  
48

### 49 **Discussion**

50  
51 In this study we investigated whether combining  $^{18}\text{F}$ -DOPA PET and multimodal MRI (with CE and  
52 PWI) improves delineation of malignant subregions in treatment-naïve enhancing and non-enhancing suspected  
53 gliomas. First, adding  $^{18}\text{F}$ -DOPA PET to multimodal MRI significantly enlarged delineated high-grade tumor  
54 volumes, substantially impacting such regions in 5 out of 16 (31%) participants. Second, in a per biopsy analysis,  
55 combined  $^{18}\text{F}$ -DOPA PET and multimodal MRI provided a sensitivity of 52% to detect high-grade tumor  
56  
57  
58  
59  
60  
61  
62  
63  
64  
65

1 subregions, compared to 41% using only multimodal MRI (with CE and PWI), without any loss of specificity  
2 (78% for both).  
3

4 **Intratumoral heterogeneity is a key issue in the management of patients with newly suspected gliomas.**  
5  
6 **Detection and delineation of malignant subregions are of major importance to target biopsies and to plan**  
7 **treatments such as surgery and/or radiation therapy.** Regarding surgical resection, obtaining complete resections  
8  
9 is the objective [2, 7]. Since, for enhancing tumors, surgical resection aims to remove all the volume with contrast  
10 enhancement, non-enhancing high-grade subregions may be unintentionally left. <sup>18</sup>F-DOPA PET and PWI can  
11 help to reveal such areas. Conversely, in non-enhancing tumors, resection extent is usually based on FLAIR  
12 hypersignal volume. If eloquent areas are included in such volume, tumor aggressiveness characterization in such  
13 subregions may help to deem acceptable or not to cause neurological damages regarding potential life-expectancy  
14 improvement [2]. Thus, to overcome limitations of conventional MRI sequences, the Response Assessment in  
15 Neuro-Oncology working group recently highlighted the potential interest of associating imaging modalities [16].  
16 Amino-acid PET relies on the overexpression of large amino acid transport systems in glial tumors, and has been  
17 demonstrated to be of interest at several time-point during the course of glioma, from the tumor characterization  
18 to the detection of relapse [8]. When comparing tumor volumes delineated with PET and standard MRI prior  
19 radiation therapy, authors reported larger volumes with amino-acid PET than with CE MRI in high-grade gliomas  
20 [17, 18], with a limited overlap (mean DSC of 0.39 to 0.56) [19, 20]. Our results are in line with these data with  
21 medians <sup>18</sup>F-DOPA<sub>VOI</sub> larger than CE<sub>VOI</sub>. The overlap between such modalities was slightly lower than previously  
22 reported data, with a median DSC of 0.28. Small volumes and limited overlaps might be explained by patient's  
23 characteristics, since in the present study emergency situations preventing <sup>18</sup>F-DOPA PET and MRI to be  
24 scheduled were exclusion criteria, the largest tumors may not have been included. Biopsy-controlled studies  
25 confirmed the improvement provided by amino-acid PET for tumor delineation in gliomas patients compared to  
26 CE MRI alone [19, 21]. Pauleit, et al. reported a sensitivity of 93% and a specificity of 94% of combined <sup>18</sup>F-  
27 FET PET/MRI to identify cellular glioma tissue [21]. When focusing on high-grade subregions detection,  
28 Pafundi, et al. reported sensitivity of 73% for <sup>18</sup>F-DOPA PET versus 27% for CE MRI alone, with 100%  
29 specificity for both [22]. These data are consistent with our results, with a sensitivity of 41% versus 28%,  
30 respectively, and a specificity of 89% for both. In retrospective survival studies, PET-guided complete resection  
31 increased the amount of anaplastic tissue removed and improved the survival of HGG patients [23], while non-  
32 resected amino-acid PET positive subregions predicted the sites of tumor progression [24]. **Recently, Laack, et**  
33 **al. reported an increased survival in glioblastoma by taking into account intratumoral heterogeneity and**  
34  
35  
36  
37  
38  
39  
40  
41  
42  
43  
44  
45  
46  
47  
48  
49  
50  
51  
52  
53  
54  
55  
56  
57  
58  
59  
60  
61  
62  
63  
64  
65

1 delivering dose-escalated radiotherapy with boost on high <sup>18</sup>F-DOPA uptake areas suggestive of malignant  
2 subregions [25].  
3

4  
5 A few studies highlighted the spatial complementarity of amino-acid PET and advanced MRI modalities.  
6  
7 Among such innovative techniques, PWI is one of the most widely used [9]. When comparing tumor volumes  
8 delineated with <sup>18</sup>F-FET PET and PWI (rCBV), PET volume has been reported to be larger than rCBV-based  
9 volume [26], with a limited overlap (median DSC of 0.37) [27]. Tietze et al. reported spatial incongruity in  
10 29% of HGG patients between rCBV maps and [<sup>11</sup>C]-methionine PET [28]. In a voxelwise analysis, Tatekawa,  
11 et al. described a significant but weak correlation (r of approximately 0.30) of intensities between <sup>18</sup>F-DOPA  
12 PET and rCBV maps [29]. In line with these results, in our study combining <sup>18</sup>F-DOPA PET with MRI including  
13 PWI substantially impacted high-grade tumor detection and/or delineation in 31% of patients. According to the  
14 per biopsy pathological validation, combining <sup>18</sup>F-DOPA PET with multimodal MRI significantly improved  
15 accuracy to 58% compared to 42% with standard MRI alone. Interestingly, the high specificity provided by  
16 combined <sup>18</sup>F-DOPA/MRI suggests that subregions highlighted by hybrid imaging should be regarded as high-  
17 grade glioma infiltration and be considered in resection planning. More broadly, such combined advanced  
18 imaging modalities may also be useful for radiation planning or biopsy targeting.  
19  
20

21  
22 Some other advanced MRI modalities have not been investigated in this study, such as diffusion-  
23 weighted imaging, MR spectroscopy and amide proton transfer imaging. These latter are less widely used [9],  
24 but might also be of additional interest for glial tumor delineation [30–33]. Moreover, emerging PET protocols  
25 such as dynamic amino-acid PET acquisitions have neither been investigated in our study [34, 35].  
26  
27

28  
29 A great variety of cut-off values are used in published studies to delineate high-grade areas in glioma,  
30 such as TBR > 1.6 [15], TBR > 2.0 [18, 22], tumor-to-striatum ratio [36] or manual contour drawing [17, 37].  
31 They all have some limitations. First, post-therapeutic changes and potential pharmacological interferences  
32 prevent cut-off values applied in progressive and/or recurrent tumors to be used at time of diagnosis [38, 39]. To  
33 date, no optimum biopsy-validated cut-off value has been established yet in glioma patients naïve to prior  
34 treatment [11, 38, 39]. Regarding tumor-to-striatum ratio, this method has been reported as less reliable since  
35 tumors and striatum do not share the same time-activity curve profile. Thus, this ratio is highly influenced by the  
36 injection-acquisition delay [39–41]. Finally, many technical considerations may explain heterogeneity across  
37 studies, such as injection-acquisition delay, spatial resolution of the PET system, presence of time-of-flight  
38 technology, reconstruction algorithms (notably the use of point-spread-function correction) and variety of  
39  
40  
41  
42  
43  
44  
45  
46  
47  
48  
49  
50  
51  
52  
53  
54  
55  
56  
57  
58  
59  
60  
61  
62  
63  
64  
65

1 methods to define the reference area. In the present study, we used a threshold value of  $TBR = 1.7$ . This value  
2 was previously reported by Patel, et al. to differentiate high-grade and low-grade glioma at the tumor scale [14].  
3

4  
5 The present study had several limitations. First, the small size of the cohort may have limited the  
6 statistical power of the analysis. Second, the absence of simultaneous PET/MRI acquisition might be regarded  
7 as a limitation, but owing to the short interval between the two examinations and the perfect post hoc registration,  
8 we considered the consequences to be negligible. Finally, based on the literature, we chose a threshold value of  
9  $rCBV > 1.6$  to define  $rCBV_{VOI}$  [15], but there is no consensus about the best  $rCBV$  threshold, and published data  
10 are highly heterogeneous, varying from 1.29 to 5.66 [41–43].  
11  
12  
13  
14  
15  
16

17 As a conclusion, adding  $^{18}F$ -DOPA PET to multimodal MRI (with CE and PWI) in patients with  
18 treatment-naïve enhancing or non-enhancing suspected gliomas substantially increased high-grade subregions  
19 delineation volume in 31% of participants. Combined  $^{18}F$ -DOPA PET/MRI enhanced accuracy for high-grade  
20 subregions detection compared to MRI alone, in a per biopsy analysis. With a high specificity, tumor subregions  
21 highlighted by hybrid imaging should be considered in treatment planning.  
22  
23  
24  
25  
26  
27  
28  
29  
30  
31  
32  
33  
34  
35  
36  
37  
38  
39  
40  
41  
42  
43  
44  
45  
46  
47  
48  
49  
50  
51  
52  
53  
54  
55  
56  
57  
58  
59  
60  
61  
62  
63  
64  
65

1  
2  
3  
4  
5  
6  
7  
8  
9  
10  
11  
12  
13  
14  
15  
16  
17  
18  
19  
20  
21  
22  
23  
24  
25  
26  
27  
28  
29  
30  
31  
32  
33  
34  
35  
36  
37  
38  
39  
40  
41  
42  
43  
44  
45  
46  
47  
48  
49  
50  
51  
52  
53  
54  
55  
56  
57  
58  
59  
60  
61  
62  
63  
64  
65

**Declarations:**

**Conflict of interest:** The authors declare that they have no conflict of interest.

**Ethics approval:** This study was validated by a national research ethics committee “CCP Ile de France 1” under number CPPIDF1-2018-ND27-cat.2 on 17<sup>th</sup> April 2018. This study was performed in accordance with the ethical standards as laid down in the 1964 Declaration of Helsinki and its later amendments.

**Funding:** This study was fully self-funded by the Eugène Marquis Center, Rennes, France. A donation of 20.000€ from the Association for the Development of Hygiene and Epidemiology in Brittany (Association pour le Developpement de l'Hygiene et de l'Epidemiologie en Bretagne: A.D.H.E.B) to the Eugène Marquis Center was dedicated to this study.

**Consent to participate:** All participants provided written and informed consent.

**Consent for publication:** All participants provided written and informed consent.

**Availability of data and material:** Data and material are available from the corresponding author on reasonable request.

**Code availability:** Not applicable.

## References

1. Ostrom QT, Bauchet L, Davis FG, et al (2014) The epidemiology of glioma in adults: a “state of the science” review. *Neuro Oncol* 16:896–913. <https://doi.org/10.1093/neuonc/nou087>
2. Weller M, van den Bent M, Preusser M, et al (2020) EANO guidelines on the diagnosis and treatment of diffuse gliomas of adulthood. *Nat Rev Clin Oncol*. <https://doi.org/10.1038/s41571-020-00447-z>
3. Almenawer SA, Badhiwala JH, Alhazzani W, et al (2015) Biopsy versus partial versus gross total resection in older patients with high-grade glioma: a systematic review and meta-analysis. *Neuro Oncol* 17:868–881. <https://doi.org/10.1093/neuonc/nou349>
4. Aum DJ, Kim DH, Beaumont TL, et al (2014) Molecular and cellular heterogeneity: the hallmark of glioblastoma. *Neurosurg Focus* 37:E11. <https://doi.org/10.3171/2014.9.FOCUS14521>
5. Scott JN, Brasher PMA, Sevick RJ, et al (2002) How often are nonenhancing supratentorial gliomas malignant? A population study. *Neurology* 59:947–949. <https://doi.org/10.1212/wnl.59.6.947>
6. Castet F, Alanya E, Vidal N, et al (2019) Contrast-enhancement in supratentorial low-grade gliomas: a classic prognostic factor in the molecular age. *J Neurooncol* 143:515–523. <https://doi.org/10.1007/s11060-019-03183-2>
7. Krivosheya D, Prabhu SS, Weinberg JS, Sawaya R (2016) Technical principles in glioma surgery and preoperative considerations. *J Neurooncol* 130:243–252. <https://doi.org/10.1007/s11060-016-2171-4>
8. Albert NL, Weller M, Suchorska B, et al (2016) Response Assessment in Neuro-Oncology working group and European Association for Neuro-Oncology recommendations for the clinical use of PET imaging in gliomas. *Neuro Oncol* 18:1199–1208. <https://doi.org/10.1093/neuonc/now058>
9. Thust SC, Heiland S, Falini A, et al (2018) Glioma imaging in Europe: A survey of 220 centres and recommendations for best clinical practice. *Eur Radiol* 28:3306–3317. <https://doi.org/10.1007/s00330-018-5314-5>
10. Delgado AF, Delgado AF (2017) Discrimination between Glioma Grades II and III Using Dynamic Susceptibility Perfusion MRI: A Meta-Analysis. *AJNR Am J Neuroradiol* 38:1348–1355. <https://doi.org/10.3174/ajnr.A5218>
11. Law I, Albert NL, Arbizu J, et al (2019) Joint EANM/EANO/RANO practice guidelines/SNMMI procedure standards for imaging of gliomas using PET with radiolabelled amino acids and [18F]FDG: version 1.0. *Eur J Nucl Med Mol Imaging* 46:540–557. <https://doi.org/10.1007/s00259-018-4207-9>
12. Plotkin M, Blechschmidt C, Auf G, et al (2010) Comparison of F-18 FET-PET with F-18 FDG-PET for biopsy planning of non-contrast-enhancing gliomas. *Eur Radiol* 20:2496–2502. <https://doi.org/10.1007/s00330-010-1819-2>
13. Wesseling P, Capper D (2018) WHO 2016 Classification of gliomas. *Neuropathol Appl Neurobiol* 44:139–150. <https://doi.org/10.1111/nan.12432>
14. Patel CB, Fazzari E, Chakhoyan A, et al (2018) 18F-FDOPA PET and MRI characteristics correlate with degree of malignancy and predict survival in treatment-naïve gliomas: a cross-sectional study. *J Neurooncol* 139:399–409. <https://doi.org/10.1007/s11060-018-2877-6>
15. Cicone F, Filss CP, Minniti G, et al (2015) Volumetric assessment of recurrent or progressive gliomas: comparison between F-DOPA PET and perfusion-weighted MRI. *Eur J Nucl Med Mol Imaging* 42:905–915. <https://doi.org/10.1007/s00259-015-3018-5>
16. Langen K-J, Galldiks N, Hattingen E, Shah NJ (2017) Advances in neuro-oncology imaging. *Nat Rev Neurol* 13:279–289. <https://doi.org/10.1038/nrneurol.2017.44>

17. Kosztyla R, Chan EK, Hsu F, et al (2013) High-grade glioma radiation therapy target volumes and patterns of failure obtained from magnetic resonance imaging and <sup>18</sup>F-FDOPA positron emission tomography delineations from multiple observers. *Int J Radiat Oncol Biol Phys* 87:1100–1106. <https://doi.org/10.1016/j.ijrobp.2013.09.008>
18. Kazda T, Pafundi DH, Kraling A, et al (2018) Dosimetric impact of amino acid positron emission tomography imaging for target delineation in radiation treatment planning for high-grade gliomas. *Phys Imaging Radiat Oncol* 6:94–100. <https://doi.org/10.1016/j.phro.2018.06.004>
19. Song S, Cheng Y, Ma J, et al (2020) Simultaneous FET-PET and contrast-enhanced MRI based on hybrid PET/MR improves delineation of tumor spatial biodistribution in gliomas: a biopsy validation study. *Eur J Nucl Med Mol Imaging*. <https://doi.org/10.1007/s00259-019-04656-2>
20. Lohmann P, Stavrinou P, Lipke K, et al (2019) FET PET reveals considerable spatial differences in tumour burden compared to conventional MRI in newly diagnosed glioblastoma. *Eur J Nucl Med Mol Imaging* 46:591–602. <https://doi.org/10.1007/s00259-018-4188-8>
21. Pauleit D, Floeth F, Hamacher K, et al (2005) O-(2-[<sup>18</sup>F]fluoroethyl)-L-tyrosine PET combined with MRI improves the diagnostic assessment of cerebral gliomas. *Brain* 128:678–687. <https://doi.org/10.1093/brain/awh399>
22. Pafundi DH, Laack NN, Youland RS, et al (2013) Biopsy validation of <sup>18</sup>F-DOPA PET and biodistribution in gliomas for neurosurgical planning and radiotherapy target delineation: results of a prospective pilot study. *Neuro Oncol* 15:1058–1067. <https://doi.org/10.1093/neuonc/not002>
23. Pirotte BJM, Levivier M, Goldman S, et al (2009) Positron emission tomography-guided volumetric resection of supratentorial high-grade gliomas: a survival analysis in 66 consecutive patients. *Neurosurgery* 64:471–481; discussion 481. <https://doi.org/10.1227/01.NEU.0000338949.94496.85>
24. John F, Bosnyák E, Robinette NL, et al (2019) Multimodal imaging-defined subregions in newly diagnosed glioblastoma: impact on overall survival. *Neuro Oncol* 21:264–273. <https://doi.org/10.1093/neuonc/noy169>
25. Laack NN, Pafundi D, Anderson SK, et al (2021) Initial Results of a Phase 2 Trial of <sup>18</sup>F-DOPA PET-Guided Dose-Escalated Radiation Therapy for Glioblastoma. *Int J Radiat Oncol Biol Phys*. 110:1383–1395. doi: 10.1016/j.ijrobp.2021.03.032
26. Filss CP, Galldiks N, Stoffels G, et al (2014) Comparison of <sup>18</sup>F-FET PET and perfusion-weighted MR imaging: a PET/MR imaging hybrid study in patients with brain tumors. *J Nucl Med* 55:540–545. <https://doi.org/10.2967/jnumed.113.129007>
27. Göttler J, Lukas M, Kluge A, et al (2017) Intra-lesional spatial correlation of static and dynamic FET-PET parameters with MRI-based cerebral blood volume in patients with untreated glioma. *Eur J Nucl Med Mol Imaging* 44:392–397. <https://doi.org/10.1007/s00259-016-3585-0>
28. Tietze A, Boldsen JK, Mouridsen K, et al (2015) Spatial distribution of malignant tissue in gliomas: correlations of <sup>11</sup>C-L-methionine positron emission tomography and perfusion- and diffusion-weighted magnetic resonance imaging. *Acta Radiol* 56:1135–1144. <https://doi.org/10.1177/0284185114550020>
29. Tatekawa H, Hagiwara A, Yao J, et al (2021). Voxelwise and Patientwise Correlation of <sup>18</sup>F-FDOPA PET, Relative Cerebral Blood Volume, and Apparent Diffusion Coefficient in Treatment-Naïve Diffuse Gliomas with Different Molecular Subtypes. *J Nucl Med* 62(3):319-325. <https://doi.org/10.2967/jnumed.120.247411>.
30. Schön S, Cabello J, Liesche-Starnecker F, et al (2020) Imaging glioma biology: spatial comparison of amino acid PET, amide proton transfer, and perfusion-weighted MRI in newly diagnosed gliomas. *Eur J Nucl Med Mol Imaging*. <https://doi.org/10.1007/s00259-019-04677-x>

- 1  
2  
3  
4  
5  
6  
7  
8  
9  
10  
11  
12  
13  
14  
15  
16  
17  
18  
19  
20  
21  
22  
23  
24  
25  
26  
27  
28  
29  
30  
31  
32  
33  
34  
35  
36  
37  
38  
39  
40  
41  
42  
43  
44  
45  
46  
47  
48  
49  
50  
51  
52  
53  
54  
55  
56  
57  
58  
59  
60  
61  
62  
63  
64  
65
31. Verburg N, Koopman T, Yaqub MM, et al (2019) Improved detection of diffuse glioma infiltration with imaging combinations: a diagnostic accuracy study. *Neuro-Oncology* noz180. <https://doi.org/10.1093/neuonc/noz180>
  32. Floeth FW, Pauleit D, Wittsack H-J, et al (2005) Multimodal metabolic imaging of cerebral gliomas: positron emission tomography with [18F]fluoroethyl-L-tyrosine and magnetic resonance spectroscopy. *J Neurosurg* 102:318–327. <https://doi.org/10.3171/jns.2005.102.2.0318>
  33. Mauler J, Maudsley AA, Langen K-J, et al (2018) Spatial Relationship of Glioma Volume Derived from <sup>18</sup>F-FET PET and Volumetric MR Spectroscopy Imaging: A Hybrid PET/MRI Study. *J Nucl Med* 59:603–609. <https://doi.org/10.2967/jnumed.117.196709>
  34. Rausch I, Zitterl A, Berroterán-Infante N, et al (2019) Dynamic [18F]FET-PET/MRI using standard MRI-based attenuation correction methods. *Eur Radiol* 29:4276–4285. <https://doi.org/10.1007/s00330-018-5942-9>
  35. Girard A, Saint-Jalmes H, Chaboub N, et al (2020) Optimization of time frame binning for FDOPA uptake quantification in glioma. *PLoS One* 15:e0232141. <https://doi.org/10.1371/journal.pone.0232141>
  36. Schwarzenberg J, Czernin J, Cloughesy TF, et al (2014) Treatment Response Evaluation Using <sup>18</sup>F-FDOPA PET in Patients with Recurrent Malignant Glioma on Bevacizumab Therapy. *Clin Cancer Res* 20:3550–3559. <https://doi.org/10.1158/1078-0432.CCR-13-1440>
  37. Rose S, Fay M, Thomas P, et al (2013) Correlation of MRI-Derived Apparent Diffusion Coefficients in Newly Diagnosed Gliomas with [ <sup>18</sup>F]-Fluoro-L-Dopa PET: What Are We Really Measuring with Minimum ADC? *AJNR Am J Neuroradiol* 34:758–764. <https://doi.org/10.3174/ajnr.A3315>
  38. Somme F, Bender L, Namer IJ, et al (2020) Usefulness of 18F-FDOPA PET for the management of primary brain tumors: a systematic review of the literature. *Cancer Imaging* 20:70. <https://doi.org/10.1186/s40644-020-00348-5>
  39. Cicone F, Carideo L, Minniti G, Scopinaro F (2019) The mean striatal 18F-DOPA uptake is not a reliable cut-off threshold for biological tumour volume definition of glioma. *Eur J Nucl Med Mol Imaging* 46:1051–1053. <https://doi.org/10.1007/s00259-019-4276-4>
  40. Chen W, Silverman DHS, Delaloye S, et al 18F-FDOPA PET Imaging of Brain Tumors: Comparison Study with 18F-FDG PET and Evaluation of Diagnostic Accuracy. 8
  41. Kudo K, Uwano I, Hirai T, et al (2017) Comparison of Different Post-Processing Algorithms for Dynamic Susceptibility Contrast Perfusion Imaging of Cerebral Gliomas. *Magn Reson Med Sci* 16:129–136. <https://doi.org/10.2463/mrms.mp.2016-0036>
  42. Abrigo JM, Fountain DM, Provenzale JM, et al (2018) Magnetic resonance perfusion for differentiating low-grade from high-grade gliomas at first presentation. *Cochrane Database Syst Rev* 1:CD011551. <https://doi.org/10.1002/14651858.CD011551.pub2>
  43. Cuccarini V, Erbetta A, Farinotti M, et al (2016) Advanced MRI may complement histological diagnosis of lower grade gliomas and help in predicting survival. *J Neurooncol* 126:279–288. <https://doi.org/10.1007/s11060-015-1960-5>

## Figure Legends

### Figure 1

Flowchart of study participants. Results in a per-biopsy analysis are presented between brackets. It should be noted that some patients diagnosed with high-grade glioma had several biopsies revealing both high-grade and low-grade subregions.

### Figure 2

Four multimodal imaging patterns of gliomas at first presentation. High-grade tumor infiltration volumes of interest obtained with  $^{18}\text{F}$ -DOPA PET (red), CE (blue) and rCBV (green) are delineated on FLAIR images on the lower line. The second and the third columns relate to patients whose high-grade glioma subregions delineation were substantially impacted by adding  $^{18}\text{F}$ -DOPA PET to multimodal MRI.

*CE, contrast enhancement,  $^{18}\text{F}$ -DOPA, [ $^{18}\text{F}$ ]-dihydroxyphenylalanine; FLAIR, fluid-attenuated inversion-recovery; mt, mutant; rCBV, regional cerebral blood volume; wt, wild-type*

### Table 1

Participants and tumor characteristics.

### Table 2

Tumor imaging characteristics.

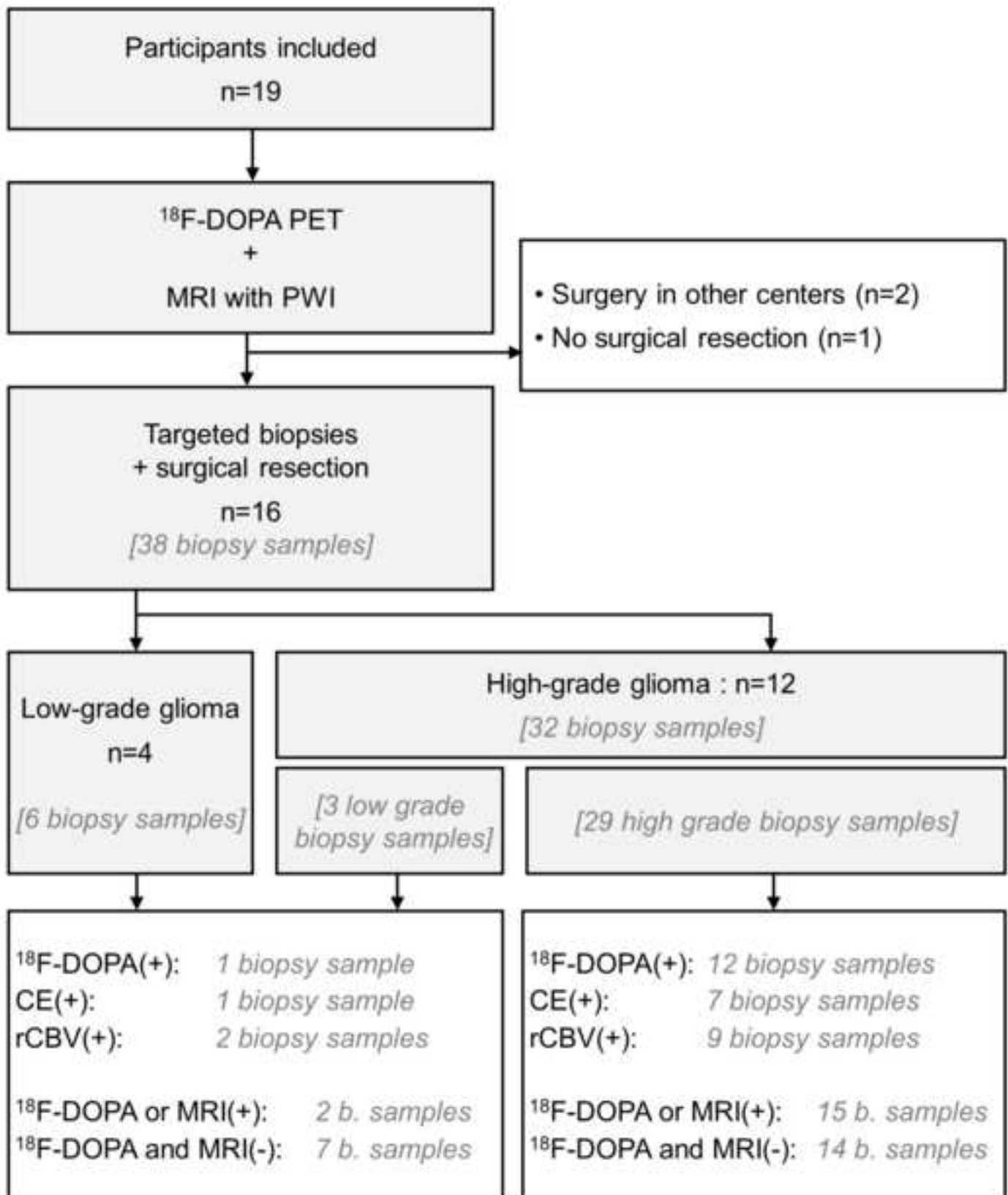
### Table 3

Diagnostic performance of each imaging modality ( $^{18}\text{F}$ -DOPA, CE and PWI) and combination (MRI and  $^{18}\text{F}$ -DOPA/MRI) for the detection of high-grade subregions of gliomas, in a per biopsy analysis.

### Supplementary Material 1

Imaging characteristics of each individual biopsy site

*CE, contrast enhancement, DOPA, [ $^{18}\text{F}$ ]-dihydroxyphenylalanine; rCBV, regional cerebral blood volume; TBR, tumor-to-normal-brain ratio*



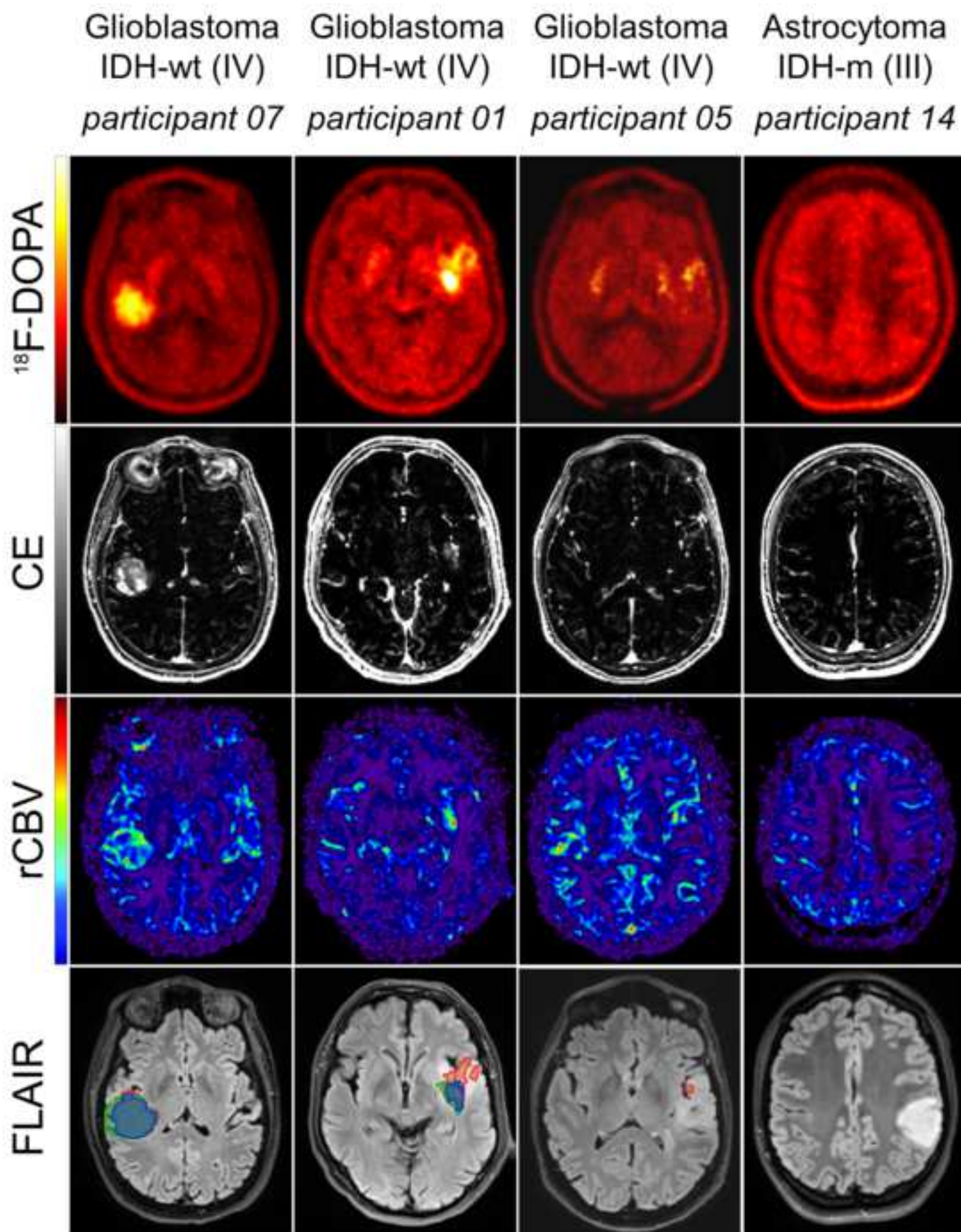


**Table 1** Participants and tumour characteristics

	n (%)
<i>Participants</i>	16
Age (years), median [interquartile range]	40 [27, 55]
Sex: men	10 (63%)
<i>Contrast-enhancement</i>	
Enhancing tumours	7 (44%)
Non-enhancing tumours	9 (56%)
<i>WHO tumour grades and types</i>	
Grade II: astrocytoma IDH-mutated	2 (12%)
oligodendroglioma IDH-mutated 1p/19q codeleted	2 (12%)
Grade III: astrocytoma IDH-mutated	6 (38%)
Grade IV: glioblastoma IDH-wild type	6 (38%)

**Table 2** Tumour imaging characteristics (bolded results highlight participants for whom adding  $^{18}\text{F}$ -DOPA PET to MRI had a substantial impact on high-grade tumour detection and/or delineation)

Part.	Age (years)	Sex	WHO type	IDH mutated	1p/19q codeleted	WHO grade	Number of biopsies	$^{18}\text{F}$ -DOPA <sub>VOI</sub> (mL)	CE <sub>VOI</sub> (mL)	rCBV <sub>VOI</sub> (mL)	MRI <sub>VOI</sub> (mL)	$^{18}\text{F}$ -DOPA/MRI <sub>VOI</sub> (mL)	$^{18}\text{F}$ -DOPA/MRI <sub>VOI</sub> - MRI <sub>VOI</sub> (mL)
01	59	M	Glioblastoma			IV	3	18.9	3.7	10.1	12.1	25.6	<b>13.5</b>
03	35	M	Astrocytoma	+		II	1	-	-	-	-	-	-
04	24	F	Oligodendroglioma	+	+	II	1	-	-	-	-	-	-
05	50	F	Glioblastoma			IV	3	0.013	-	-	-	0.013	<b>0.013</b>
06	24	M	Astrocytoma	+		III	2	0.12	0.74	61.7	62.5	62.5	0.0
07	58	F	Glioblastoma			IV	2	12.6	15.5	21.1	21.8	21.9	0.1
08	67	M	Glioblastoma			IV	2	9.4	4.7	13.5	14.9	17.3	<b>2.4</b>
09	37	M	Astrocytoma	+		II	1	-	-	-	-	-	-
10	43	M	Astrocytoma	+		III	3	18.3	0.90	0.30	1.2	18.5	<b>17.3</b>
12	26	M	Astrocytoma	+		III	3	-	-	-	-	-	-
13	27	M	Astrocytoma	+		III	3	10.6	16.1	10.0	20.6	21.4	0.8
14	23	F	Astrocytoma	+		III	2	-	-	-	-	-	-
15	42	F	Astrocytoma	+		III	3	0.20	0.054	1.4	1.5	1.7	0.2
16	54	M	Glioblastoma			IV	3	-	-	-	-	-	-
18	32	F	Oligodendroglioma	+	+	II	3	-	-	1.8	1.8	1.8	0.0
19	63	M	Glioblastoma			IV	3	3.4	-	3.1	3.1	6.0	<b>3.0</b>
Median [inter-quartile range]								0.07	0.0	0.9	1.3	1.7	

Note : “-“ represents null volumes

**Table 3** Diagnostic performance of each imaging modality ( $^{18}\text{F}$ -DOPA, CE and PWI) and combination (MRI and  $^{18}\text{F}$ -DOPA/MRI) for the detection of high-grade subregions of gliomas, in a per biopsy analysis

	<b>CE(+)</b>	<b>PWI(+)</b>	<b>MRI(+)</b> <b>(CE(+) and/or PWI(+))</b>	<b><math>^{18}\text{F}</math>-DOPA(+)</b>	<b><math>^{18}\text{F}</math>-DOPA/MRI(+)</b>
Accuracy	42% (16/38)	42% (16/38)	50% (19/38)	53% (20/38)	58% (22/38)
[95% confidence interval]	[26%, 58%]	[26%, 58%]	[34%, 66%]	[37%, 69%]	[41%, 74%]
Sensitivity	28% (8/29)	31% (9/28)	41% (12/29)	41% (12/29)	52% (15/29)
[95% confidence interval]	[13%, 47%]	[15%, 51%]	[24%, 61%]	[24%, 61%]	[33%, 71%]
Specificity	89% (8/9)	78% (7/9)	78% (7/9)	89% (8/9)	78% (7/9)
[95% confidence interval]	[52%, 100%]	[40%, 97%]	[40%, 97%]	[52%, 100%]	[40%, 97%]

*Legend: CE, contrast enhancement,  $^{18}\text{F}$ -DOPA, [ $^{18}\text{F}$ ]-dihydroxyphenylalanine; PWI, perfusion-weighted imaging*

